Identifying Hydroxyls on the TiO2 (110)−1 × 1 Surface with Scanning Tunneling Microscopy

ARTICLE *in* THE JOURNAL OF PHYSICAL CHEMISTRY C · JULY 2009

Impact Factor: 4.77 · DOI: 10.1021/jp901657u

Identifying Hydroxyls on the TiO_2 (110)−1 × 1 Surface with Scanning Tunneling Microscopy

Xuefeng Cui, Zhuo Wang, Shijing Tan, Bing Wang,* Jinlong Yang, and J. G. Hou*

Hefei National Laboratory for Physical Sciences at the Microscale, University of Science and Technology of China, Hefei, Anhui 230026, P. R. China

Received: February 23, 2009; Revised Manuscript Received: June 16, 2009

We present the investigations of hydroxylated TiO_2 (110)−1 × 1 surfaces using scanning tunneling microscopy (STM). It is observed that in topographic images the protrusions of hydroxyls (OH) on TiO_2 (110) surfaces are dependent on the tip−sample distance in STM measurements at room temperature. In comparison with those of the fivefold coordinated Ti atoms and the oxygen vacancies, the relative apparent height of OHs becomes smaller and smaller with decreasing tip−sample distance by changing the imaging conditions. The OHs even become invisible in much shorter tip−sample distances. Reversibly, the OHs are almost completely recovered when the imaging conditions are restored. It suggests that the OHs may be identified by varying the imaging conditions in STM measurement.

Introduction

Rutile TiO_2 (110) has become a widely studied oxide surface, and it has been used to model the TiO_2 catalytic properties under ultrahigh vacuum (UHV) conditions.[1−13] Scanning tunneling microscopy (STM) is a powerful tool to provide an excellent prospect for imaging chemical reactions with atomic resolution.[5,10,12,14−16] Detailed understanding and controlling at the atomistic level of the nature of adsorbates and their reactions in oxide surfaces are essential for understanding of their catalytic properties. The problem is that the common point defects present on the surface, such as oxygen vacancies (O_V) and hydroxyl (OH) impurities, are often elusive species.[10,11,17] O_V's are intrinsic point defects in the partially reduced TiO_2 (110)−1 × 1 surface, while OHs are generally the dissociation products of water in the oxygen vacancies of the surface, even in UHV systems, and therefore difficult to avoid.[3,5,9−11,17] Both O_V and OH defects show up as bright protrusions, as do most of the other adsorbed molecules in normal STM images.[2] Thus, it is an important issue to distinguish the point defects of the O_V and OH from the adsorbed molecules being studied. One method is to apply high bias voltages (>3 V) to remove OH experimentally in STM measurements.[5,9] However, this method may also affect the concerned adsorbed molecules, making it in limited applications. Instead, we recently found that the O_V and the OH can be recognized by comparing their occupied state and the empty state images.[18] Its limitation is that the occupied state image is difficult to be acquired due to the low conductance of TiO_2 at negative bias. A very complicated method by combination of atomic force microscopy and STM was demonstrated recently by Enevoldsen et al.[7]

In this paper, we investigate the hydroxylated TiO_2 (110)−1 × 1 surface using a combined experimental and theoretical study. We find that the protrusions of hydroxyls vary with tip−sample distance at room temperature. At bias voltages lower than 1.6 V, when the STM tip gets closer and closer to the sample by either increasing the set point current or decreasing the bias voltage, the OHs become less and less protruded, and even become invisible in STM images. However, when the tip gets back, the protruded OHs are recovered. This phenomenon is quite reversible and highly reproducible, which indicates that the OHs remain on the surface. Comparing with the images of coadsorption of OHs and methanol molecules, we observed that only the OHs have such imaging condition dependence, suggesting that this method can be used to identify the OHs from other adsorbates in STM measurement.

Experimental Section

The experiments were conducted with a variable temperature scanning tunneling microscope (Omicron, MATRIX) in an ultrahigh vacuum (UHV) system, which was baked for about 100 h and had a base pressure greater than 3×10^{-11} torr. A one-side polished rutile TiO_2 (110) sample ($10 \times 5 \times 0.5$ mm^3, Princeton Scientific) was prepared by more than 10 cycles of sputtering with 1000 eV Ar^+ ions for about 15 min, followed by annealing at 900 K (heated by a Ta-foil heater behind the sample mounted on the Omicron's sample plate) for about 30 min in each cycle. With this method, nearly hydroxyl-free TiO_2 (110)−1 × 1 surface was obtained.[19] The partially hydroxylated TiO_2 (110)−1 × 1 surface was obtained by keeping the freshly prepared sample in UHV for about 8 h to have it hydroxylated from the residual water in UHV. The fully hydroxylated TiO_2 (110)−1 × 1 surface was prepared by dosing water through a conducting tube directly to the sample surface at room temperature. To minimize exposure of water into the chamber, the distance between the tube outlet and the sample surface was about 3−5 mm. The STM measurements were performed with a constant current mode at room temperature. The chemically etched tungsten tip was carefully cleaned before use.

Theoretical Calculations

A TiO_2 (110)−1 × 1 surface was modeled by periodically repeated slabs consisting of a (6 × 2) cell with 5 Ti layers separated by 10 Å of vacuum. Our calculations were conducted by using the Vienna ab initio simulation package code (VASP)[20−22] with the generalized gradient approximation of Perdew, Burke, and Ernzerhof (PBE-GGA).[23] The projector

* To whom correspondence should be addressed. E-mail: bwang@ustc.edu.cn (B.W); jghou@ustc.edu.cn (J.G.H).

10.1021/jp901657u CCC: $40.75
Published on Web 07/02/2009

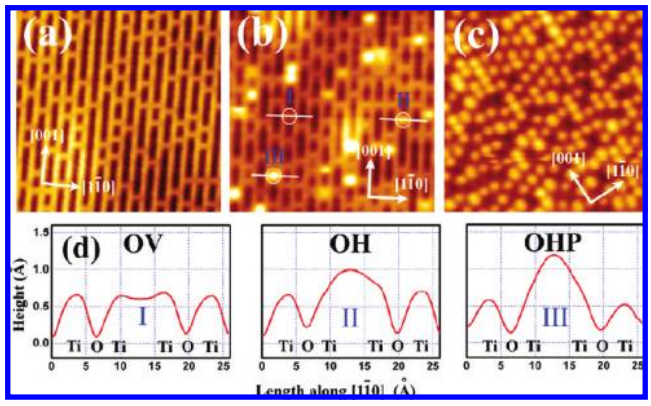

Figure 1. STM images of (a) hydroxyl-free, (b) partially hydroxylated, and (c) fully hydroxylated TiO_2(110)−1 × 1 surfaces recorded at room temperature. Size, 11 × 11 nm^2; imaging conditions of 1.6 V and 10 pA. (d) Line profiles from the labeled site in (b) for O_V, OH, and OHP, respectively.

augmented wave (PAW) potential was employed.[24,25] Monhkorst-3 Pack grids of (2 × 2 × 1) K-points were used for the (2 × 6) unit cells. During the optimization, atoms were allowed to relax in the uppermost two layers until the force acting on each became less than 0.02 eV Å^{-1}. The energy cutoffs for the plane waves were 400 eV. STM images were simulated by the Tersoff−Hamann approach.[26,27]

Results and Discussion

Parts a−c of Figure 1 show STM images of hydroxyl-free, partially hydroxylated, and fully hydroxylated TiO_2(110)−1 × 1 surfaces, respectively. In the hydroxyl-free surface (Figure 1a), the bright and dark parallel rows represent the fivefold coordinated Ti atoms (Ti_{5c}) and bridging oxygen atoms (O_{br}), respectively. The bright protrusions in O_{br} rows are the oxygen vacancies (O_V). The O_V concentration is about 10%. Before water dosing, the hydroxyl-free surface is able to be maintained for about 1−2 h with only less than 5−10 OHs in an area of 100 × 100 nm^2 from the residual background water of the UHV chamber. In the partially hydroxylated surface (Figure 1b), three types of bright protrusions are observed. These protrusions are attributed to O_V's, OHs, and OH pairs (OHP), respectively. The OHP is more protruded than the OH. Their relative apparent heights are shown in Figure 1d, which is a typical behavior observed before.[16] In the fully hydroxylated surface (Figure 1c), all of the O_V's are covered with OHs. Estimated OH concentration based on total areas of ∼100 nm^2 is about 19%. The OH concentration is almost doubled compared with the O_V concentration, indicating that the OHs are the product of dissociated water.[5]

Figure 2 shows a series of STM images of a partially hydroxylated surface under various imaging conditions. All of the images exhibit the same area. At a low tunneling current (say, in a range of 1−50 pA), OHs are more protruded than O_V's. However, it is observed that with increased tunneling current, the OHs become faint, and even invisible (Figure 2a_4 and a_5). At 1.2 V, the OHs are nearly invisible when the tunneling current increases to about 200 pA. At 1.6 V, the OHs become invisible only when the tunneling current gets up to about 600 pA. In all of the measured images, the O_V's are always observable. As shown in Figure 2a_4 and b_4, the OHs can become invisible by decreasing the bias voltage from 1.6 to 1.2 V at the same tunneling current of 300 pA.

The OHs can be visible again if we decrease the tunneling current or increase the bias voltage. As shown in Figure 2a_6 and b_6, we observe nearly the same features as the original ones after a series of images are acquired at higher currents. The phenomenon is quite reversible and reproducible. In several cycles of measurements, most of the OHs are present at their original positions. At room temperature, the hopping rate of H on TiO_2(110)−1 × 1 is about 10^{-5} s^{-1}[3]. It means that one may only observe the event of H diffusion less than several percent per hour. Our observation is in good agreement with the result by Li et al. at room temperature.[3] Our observation also suggests that an individual STM image acquired at certain conditions may be insufficient to determine whether a TiO_2(110)−1 × 1 surface is hydroxyl-free or not.

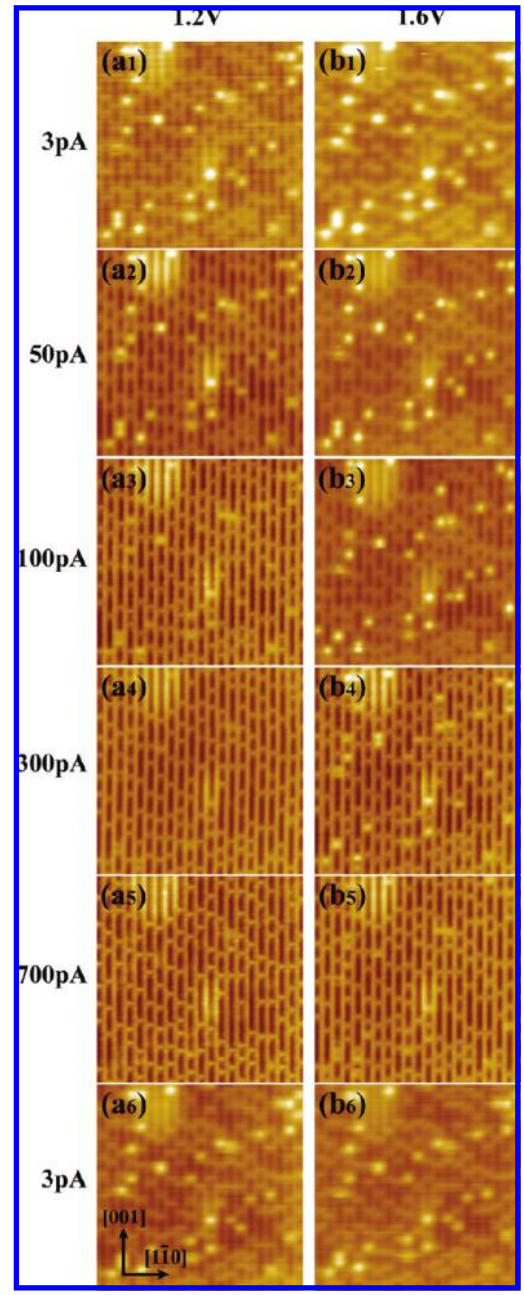

Figure 2. STM images (14 × 14 nm^2) of the partially hydroxylated TiO_2(110)−1 × 1 surface within the same area at various imaging conditions at room temperature. Acquisition sequence: a_1 → a_6 → b_1 → b_6.

High resolution STM images of a single OH and an OHP are given in Figure 3. At a high tunneling current of 700 pA (Figure 3a_2 and b_2), the OH is almost invisible, while the OHP

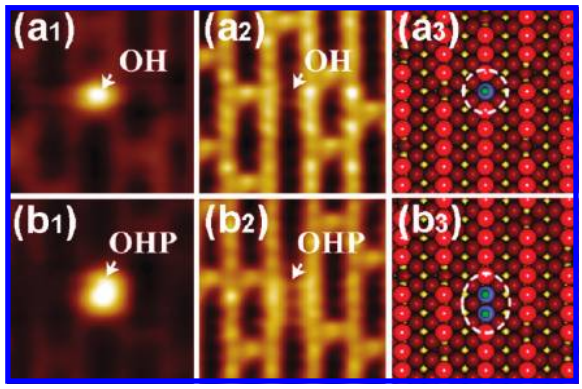

Figure 3. High resolution STM images of TiO_2 (110) surface with a single OH and an OHP recorded at (a_1 and b_1) 1.2 V, 10 pA, (a_2 and b_2) 1.2 V, 700 pA. Size: 30 × 30 Å^2. (a_3 and b_3) Schematic ball models of the areas, respectively.

is still faintly visible but much less protruded than O_V. The OHs and the OHPs have the similar trend to become faint and even invisible with increasing the tunneling current or decreasing the bias voltage. The schematic ball models of the scanning areas are respectively given in Figure $3a_3$ and b_3. The dashed circle and ellipse indicate the positions of the hydroxyl and the hydroxyl pair (OHP), respectively.

Figure 4 shows consecutively acquired STM images for the fully hydroxylated surface within the same area. Since all of the O_V's are occupied by OHs, there is no O_V in the images. A similar phenomenon is observed for the OHs with various imaging conditions. At a low current of 5 pA (Figure 4a), the protrusions reflect the OHs, which are located on the O_{br} rows.[10,11] The Ti_{5c} rows are less pronounced. With increasing of the tunneling current, the OHs become faint, and the Ti_{5c} rows become much more pronounced (Figure 4b and c). At a condition of 500 pA, only the Ti_{5c} rows are visible in the image (Figure 4d). With reversely decreasing the tunneling current, the OHs are visible again (Figure 4e and f). The behaviors for OHs by changing the bias are similar to the observations for the partially hydroxylated surface in Figures 2 and 3.

Considering the experimental observations above that visible or invisible behaviors of OHs are fairly dependent on the imaging conditions and highly reversible, we believe that the OHs remain on the $TiO_2(110)-1 \times 1$ surfaces during the STM image acquisitions. Similar behavior has been observed before.[8,9,28] It is mainly attributed to the dependence of the tip structure[28] or chemical composition at the tip apex.[8] However, it is difficult to explain our observations shown above. Such invisible OH species acquired at lower bias voltages, typically smaller than 2.5 V, should be different from the case of OH dehydrogenation at high bias voltages (>3 V).[5,9]

With various imaging conditions, the change of the OH behaviors can be mainly related to the change of tip−sample distance. With increased tunneling current or decreased bias voltage, the STM tip becomes closer to the sample. A closer tip−sample distance causes a much fainter or even invisible image of OHs, and vice versa. However, an OH bond on the $TiO_2(110)-1 \times 1$ surface is generally considered to be orientated perpendicularly to the (110) plane.[3,10,11,17,29] With such configuration, our simulation shows that the OH always exhibits as a protrusion independent of the tip−sample distance, in agreement with previous simulations,[16] but it is still difficult to explain the OH contrast dependence on the tip−sample distance in our observations.

In the observation by Suzuki et al., the OH is visible at the conditions of 300 pA and 2.5 V, but the OH becomes invisible at the conditions of 300 pA and 1.0 V.[9] In their experiment, they used a relatively high bias of 2.5 V. In general, while keeping tunneling current, a higher bias gives a larger tip−sample distance, and vice versa. The tunneling current in several hundreds pA is not a sufficient condition to see the OHs. To avoid dehydrogenation at a high bias voltage,[5] we here demonstrate that the similar phenomenon happens at relatively low biases of 1.2 and 1.6 V with varying current. As shown in Figure 2, in theses two sets of biases the images of OHs were obtained reversibly. Moreover, it shows that the OH can still be visible at 300 pA and 1.6 V, but almost invisible or distinguishable at 300 pA but a lower bias of 1.2 V (Figure $2a_4$ and b_4). In principle, our observations are in good agreement with the results by Suzuki et al.,[9] suggesting the contrast dependence of OHs on the tip−sample distance.

A recent calculation revealed that OH at bridging O is tilted in the $[1\bar{1}0]$ direction, which is the most stable species.[13] We thus suppose that the OH bond may orientate tilting from the normal direction with decrease of the tip−sample distance. Decreasing the tip−sample distance causes the increase of the electric field between the tip and the sample. The OH bond may thus further tilt from the normal direction under high enough electric field when the tip gets closer to the surface.

To support our suggestion, we make simulations for OH with various orientations on the TiO_2 (110) surface using a slab model of a 6 × 2 unit cell with 5 Ti layers.[19] Figure 5 shows the simulated images with their schematic models for the OH bond normal and parallel to the (110) surface. When the OH bond orientates normal to the surface, the OH is always observable and more protruded than Ti_{5c} atoms in the image (Figure 5a). When the OH bond orientates parallel to the surface along either the $[1\bar{1}0]$ or [001] direction, the OH is invisible in both cases (Figure 5b and c). An OHP gives the similar invisible image in the simulation (Figure 5d). The simulated images well support our assumption. The energy difference between the bent and straight up OH groups is about 0.015 eV, which may be a reasonable alternate for OH groups between bent and straight up by changing of the tip−sample distance.

It is noted that when the OH (Figure 5b) or OHP (Figure 5d) is tilted toward the $[1\bar{1}0]$ direction, the Ti_{5c} atoms on the one side which is close to hydrogen appear brighter than the Ti_{5c} atoms on the other side. Experimentally, such unsymmetrical brightness of Ti_{5c} atoms near the OH or OHP is likely observable, as shown in Figure $3a_2$ and b_2. However, it should be pointed out that in theses cases the situations of O_V are different for the Ti_{5c} row from one side to the other side. From our simulations, the contrast of such unsymmetrical brightness of Ti_{5c} atoms near the OH or OHP is relatively slight, which may not be remarkably exhibited and may be affected by the O_V environment in our experiment.

The dependence of OH contrast on tip−sample distance may be used to identify OH from other adsorbates. Figure 6 gives two sets of images, showing coadsorption of methanol and OH under different imaging conditions. In the set of Figure 6a−c, the adsorbates exhibit as protrusions with nearly the same contrast under the acquisition conditions of 1.6 V and 5 pA (Figure 6a); by increasing the tunneling current to 600 pA some of the adsorbates become almost invisible, while some other adsorbates remain protruded, for instance, as correspondingly marked sites in the dashed rectangle in Figure 6a. The invisible adsorbates can be restored if we set back the imaging conditions to 1.6 V and 5 pA. Based on the behavior of OH discussed above, we may thus assign the nearly invisible protrusions in Figure 6b to OHs, while the remaining protrusions are assigned

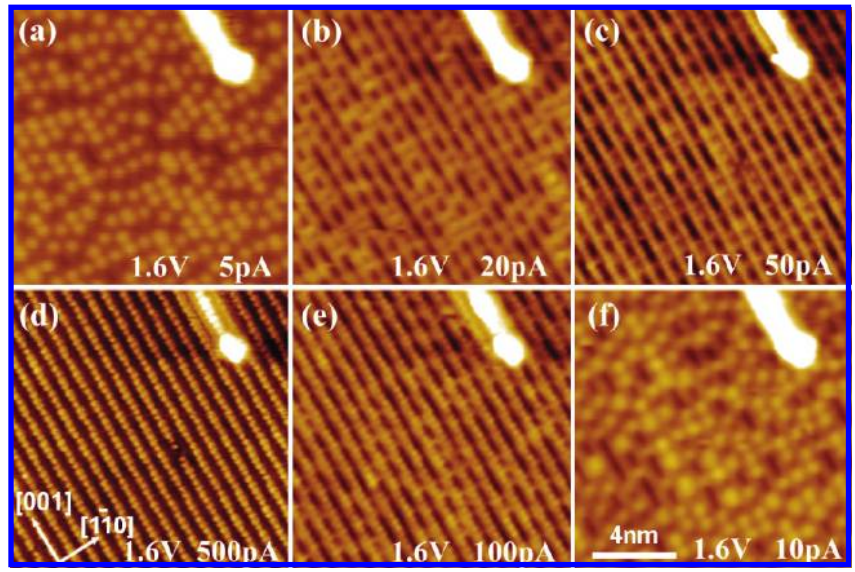

Figure 4. Consecutively acquired STM images for the fully hydroxylated TiO_2(110)−1 × 1 surface at room temperature: (a) 5, (b) 20, (c) 50, (d) 500, (e) 100, and (f) 10 pA, while keeping bias voltage at 1.6 V. Size: 14 × 14 nm^2.

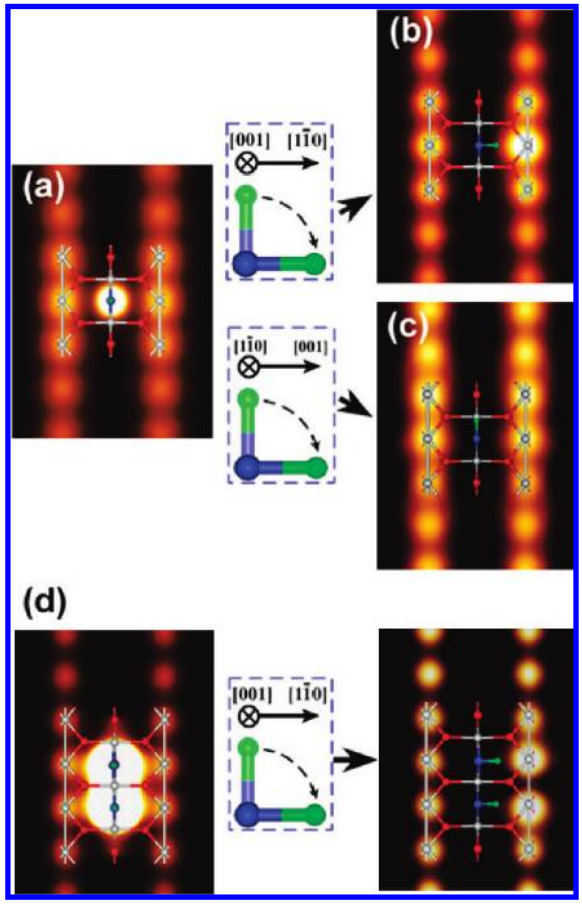

Figure 5. Simulated empty state STM images (sample bias 0.8 V at constant height of 3.0 Å) with superposed ball−stick models for (a) normal orientated OH, (b) parallel orientated OH to the (110) surface along the [1$\bar{1}$0] direction, (c) parallel orientated OH to the (110) surface along the [001] direction, (d) normal orientated OHP (left) and parallel orientated OHP along the [1$\bar{1}$0] direction (right). The tilting directions of OH are schematically given.

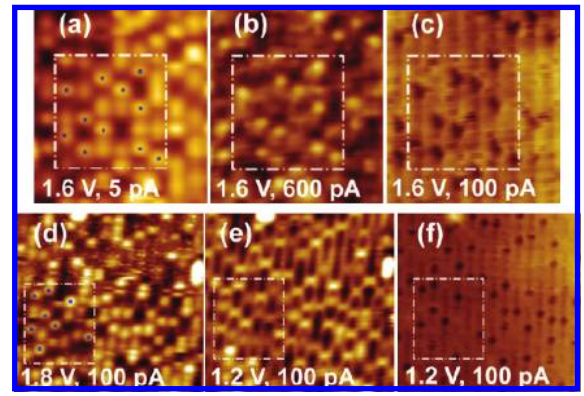

Figure 6. STM images of coadsorption of methanol and OHs on TiO_2(110)−1 × 1 with different imaging conditions, as labeled in images. (a−c) Size: 5.9 × 6.7 nm^2. (d−f) Size: 11 × 11 nm^2. (c and f) Images acquired with spontaneously decorated tips, respectively.

to the methoxy species due to dissociative adsorption of methanol.[4] This is confirmed by a spontaneously decorated tip acquired at the same area, as shown in Figure 6c. The imaged black holes in Figure 6c correspond well to the remaining protrusions in Figure 6b. Hence, the still visible protrusions in Figure 6b can be assigned to the methoxy species. Such phenomenon of resolvable methoxy species with the decorated tip has been observed before by Zhang et al.[4] The decoration is most likely attributed to the methanol or methoxy species at the tip apex. In another set of Figure 6d−f, by changing the bias from 1.8 to 1.2 V while keeping a tunneling current of 100 pA, we observe similar behaviors of remaining protrusions of methoxy species and OHs becoming invisible. In both of these two sets of measurements by changing tunneling current or bias voltage, the dependence of OH contrast on tip−sample distance remains even though there exist methoxy species on the surface. The observations for coadsorption of methanol molecules and OHs suggest that it may be an easy way to identify the OHs from the other adsorbates, for instance, methoxy species, by changing the tip−sample distance.

During revision of this manuscript, we noticed that in a recent work by Enevoldsen et al. the on-top H of the surface OH may be pushed to a subsurface site by a tip with noncontact atomic force microscopy (nc-AFM), forming subsurface OH groups (OH_{sub}) in a stable interstitial site.[30] They revealed that the energy barrier for the OH_{sub} to jump back to the surface and form a bridging OH is ∼2 eV, which is sufficiently high to block spontaneous back-diffusion of H at room temperature;

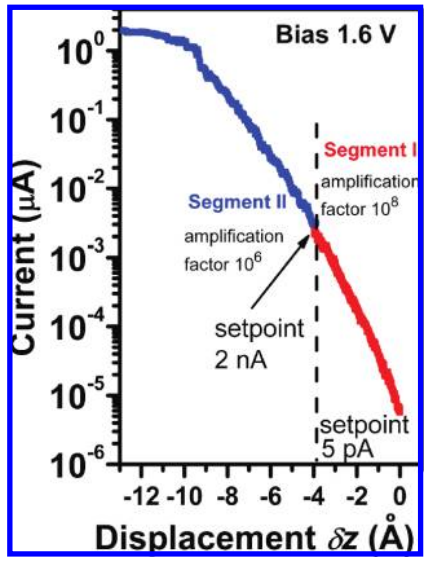

Figure 7. Typical $I-z$ curve obtained in two segments with selected amplification factors of 10^8 and 10^6 of a preamplifier (DLPCA-200, FEMTO). The initial set point conditions are 1.6 V and 5 pA (segment I) and 1.6 V and 2 nA (segment II). The occurrence of saturated current value of about 2 μA is correlated with the contact of the tip with the sample surface, leading to a tip−sample distance of 9.3 Å at 1.6 V and 5 pA.

thus, the OH_{sub} is irreversible. In contrast, the energy for a bent OH is higher than that for a straight up OH by only 0.015 eV; thus, reversible behavior of OH can be observed. With the measurement of the current−height ($I-z$) curves by pushing the tip to contact with the surface, we have determined the tip−sample distance, for instance, of about 9.3 Å at 1.6 V and 5 pA, as shown in Figure 7 by a typical $I-z$ curve. The change of the tip−sample distance is about 2.6 Å by setting imaging conditions from 1.6 V and 5 pA to 1.6 V and 500 pA. In this case, the tip is still far from the surface by about 6.7 Å. Hence, the bend of OH may not be directly pushed by the tip, but most likely due to the electric field change.

Conclusion

In summary, we have studied the morphologies of hydroxyl groups on the TiO_2 (110)−1 × 1 surface with different imaging conditions and compared them with those of adsorbed methanol molecules. We find that by decreasing the tip−sample separation through the sample bias and tunneling current, the OHs in STM images may change from bright protrusions to faint, and even invisible. This behavior may be attributed to the OH bond tilting under a high electric field when the STM tip gets closer to the TiO_2 surface. Simulated STM images well support our suggestion. By comparing with the coadsorbed methanol molecules, we find that only the OHs have such OH contrast dependence on the tip−sample separation, while the methoxy species remain as bright protrusions with different imaging conditions. It suggests that such behaviors of OH may be used to experimentally distinguish OH from other adsorbates on the TiO_2 surface, which may be a useful technique to identify the physical and chemical properties of hydroxylated TiO_2 surfaces.

Acknowledgment. This work was supported by the NSFC (Grant Nos. 50721091, 10825415, 60771006, 50532040) and NBRP (Grant No. 2006CB922001), China.

References and Notes

(1) Henderson, M. A. *Surf. Sci. Rep.* **2002**, *46*, 1.
(2) Diebold, U. *Surf. Sci. Rep.* **2003**, *48*, 53.
(3) Li, S. C.; Zhang, Z. R.; Sheppard, D.; Kay, B. D.; White, J. M.; Du, Y.; Lyubinetsky, I.; Henkelman, G.; Dohnalek, Z. *J. Am. Chem. Soc.* **2008**, *130*, 9080.
(4) Zhang, Z. R.; Bondarchuk, O.; White, J. M.; Kay, B. D.; Dohnalek, Z. *J. Am. Chem. Soc.* **2006**, *128*, 4198.
(5) Bikondoa, O.; Pang, C. L.; Ithnin, R.; Muryn, C. A.; Onishi, H.; Thornton, G. *Nat. Mater.* **2006**, *5*, 189.
(6) Brookes, I. M.; Muryn, C. A.; Thornton, G. *Phys. Rev. Lett.* **2001**, *87*, 266103.
(7) Enevoldsen, G. H.; Foster, A. S.; Christensen, M. C.; Lauritsen, J. V.; Besenbacher, F. *Phys. Rev. B* **2007**, *76*, 205415.
(8) Enevoldsen, G. H.; Pinto, H. P.; Foster, A. S.; Jensen, M. C. R.; Kühnle, A.; Reichling, M.; Hofer, W. A.; Lauritsen, J. V.; Besenbacher, F. *Phys. Rev. B* **2008**, *78*, 045416.
(9) Suzuki, S.; Fukui, K.; Onishi, H.; Iwasawa, Y. *Phys. Rev. Lett.* **2000**, *84*, 2156.
(10) Wendt, S.; Matthiesen, J.; Schaub, R.; Vestergaard, E. K.; Lægsgaard, E.; Besenbacher, F.; Hammer, B. *Phys. Rev. Lett.* **2006**, *96*, 066107.
(11) Wendt, S.; Schaub, R.; Matthiesen, J.; Vestergaard, E. K.; Wahlström, E.; Rasmussen, M. D.; Thostrup, P.; Molina, L. M.; Lægsgaard, E.; Stensgaard, I.; Hammer, B.; Besenbacher, F. *Surf. Sci.* **2005**, *598*, 226.
(12) Wendt, S.; Sprunger, P. T.; Lira, E.; Madsen, G. K. H.; Li, Z. S.; Hansen, J. Ø.; Matthiesen, J.; Blekinge-Rasmussen, A.; Lægsgaard, E.; Hammer, B.; Besenbacher, F. *Science* **2008**, *320*, 1755.
(13) Yin, X. L.; Calatayud, M.; Qiu, H.; Wang, Y.; Birkner, A.; Minot, C.; Wöll, C. *Chem. Phys. Chem.* **2008**, *9*, 253.
(14) Besenbacher, F.; Lauritsen, J. V.; Wendt, S. *Nano Today* **2007**, *2*, 30.
(15) Maksymovych, P.; Mezhenny, S.; Yates, J. T. *Chem. Phys. Lett.* **2003**, *382*, 270.
(16) Teobaldi, G.; Hofer, W. A.; Bikondoa, O.; Pang, C. L.; Cabailh, G.; Thornton, G. *Chem. Phys. Lett.* **2007**, *437*, 73.
(17) Zhang, Z.; Bondarchuk, O.; Kay, B. D.; White, J. M.; Dohnalek, Z. *J. Phys. Chem. B* **2006**, *110*, 21840.
(18) Minato, T.; Sainoo, Y.; Kim, Y.; Kato, H. S.; Aika, K.-i.; Kawai, M.; Zhao, J.; Petek, H.; Huang, T.; He, W.; Wang, B.; Wang, z.; Zhao, Y.; Yang, J.; Hou, J. G. *J. Chem. Phys.* **2009**, *130*, 124502.
(19) Cui, X. F.; Wang, B.; Wang, Z.; Huang, T.; Zhao, Y.; Yang, J. L.; Hou, J. G. *J. Chem. Phys.* **2008**, *129*, 044703.
(20) Kresse, G.; Hafner, J. *Phys. Rev. B* **1993**, *48*, 13115.
(21) Kresse, G.; Hafner, J. *Phys. Rev. B* **1993**, *47*, 558.
(22) Kresse, G.; Hafner, J. *Phys. Rev. B* **1994**, *49*, 14251.
(23) Perdew, J. P.; Wang, Y. *Phys. Rev. B* **1992**, *45*, 13244.
(24) Kresse, G.; Joubert, D. *Phys. Rev. B* **1999**, *59*, 1758.
(25) Lindan, P. J. D.; Harrison, N. M.; Gillan, M. J.; White, J. A. *Phys. Rev. B* **1997**, *55*, 15919.
(26) Tersoff, J.; Hamann, D. R. *Phys. Rev. Lett.* **1983**, *50*, 1998.
(27) Tersoff, J.; Hamann, D. R. *Phys. Rev. B* **1985**, *31*, 805.
(28) Diebold, U.; Lehman, J.; Mahmoud, T.; Kuhn, M.; Leonardelli, G.; Hebenstreit, W.; Schmid, M.; Varga, P. *Surf. Sci.* **1998**, *411*, 137.
(29) Valentin, C. D.; Pacchioni, G.; Selloni, A. *Phys. Rev. Lett.* **2006**, *97*, 166803.
(30) Enevoldsen, G. H.; Pinto, H. P.; Foster, A. S.; Jensen, M. C. R.; Hofer, W. A.; Hammer, B.; Lauritsen, J. V.; Besenbacher, F. *Phys. Rev. Lett.* **2009**, *102*, 136103.

JP901657U